General Disclaimer

One or more of the Following Statements may affect this Document

- This document has been reproduced from the best copy furnished by the organizational source. It is being released in the interest of making available as much information as possible.

- This document may contain data, which exceeds the sheet parameters. It was furnished in this condition by the organizational source and is the best copy available.

- This document may contain tone-on-tone or color graphs, charts and/or pictures, which have been reproduced in black and white.

- This document is paginated as submitted by the original source.

- Portions of this document are not fully legible due to the historical nature of some of the material. However, it is the best reproduction available from the original submission.

NASA TECHNICAL MEMORANDUM

NASA TM-78886

NASA TM-78886

VARIATION OF FAN TONE STEADINESS FOR SEVERAL INFLOW CONDITIONS

by J. R. Balombin
Lewis Research Center
Cleveland, Ohio 44135

TECHNICAL PAPER to be presented at the
Eleventh Fluid and Plasma Dynamics Conference
sponsored by the American Institute of
Aeronautics and Astronautics
Seattle, Washington, July 10-12, 1978

VARIATION OF FAN TONE STEADINESS FOR SEVERAL INFLOW CONDITIONS

by J. R. Balombin

National Aeronautics and Space Administration
Lewis Research Center
Cleveland, Ohio 44135

Abstract

An amplitude probability density function analysis technique for quantifying the degree of fan noise tone steadiness has been applied to data from a fan tested under a variety of inflow conditions. The test conditions included typical static operation, inflow control by a honeycomb/screen device and forward velocity in a wind tunnel simulating flight. The ratio of mean square sinusoidal-to-random signal content in the fundamental and second harmonic tones was found to vary by more than an order-of-magnitude. Some implications of these results concerning the nature of fan noise generation mechanisms are discussed.

E-9621

Introduction

Consciousness of the extensive differences in fan noise between operation under flight conditions and under ground static conditions has become widespread, and the phenomenon has been under study for several years. The noise levels of the blade passage tone are observed to decrease when the fan is operated at flight conditions; the levels of cut-on tones have also been observed to become more steady in flight. References such as 1, 2, and others have detailed these effects. In trying to simulate flight behavior of fan noise during ground testing, the approach has been to test at ground static conditions with added screens or honeycomb flow straighteners upstream of the fan inlet. These inlet flow control devices have been observed to reduce the level of in-flow turbulence and fan tones.

Testing that covers the effect of a honeycomb/screen ahead of a fan, and also the effect of tunnel flow in simulating forward flight operation was performed at NASA's Lewis Research Center and the results presented at the AIAA 4th Aeroacoustic Conference.[3] Substantial reduction of the inlet fundamental fan tone was achieved with tunnel flow. A lesser reduction of the tone level was achieved with the simple addition of a honeycomb/screen device during static testing in the same facility.[4] The present paper analyzes these results in more detail.

In particular, attention is paid to measures of the variability of the fan tone noise with time. The actual level of the blade passage frequency tone is recognized to vary significantly with time by amounts ranging well over 10 dB. The unsteadiness of these tones can be appreciated by studying time histories of the mean square level as recorded by an x-y plotter. The measured time variations seem to be a strong function of the testing environment, as evidenced by the fact that flight test results do not exhibit this same unsteadiness. In fact, cut-on fan tones during flight testing have been observed to be very steady in amplitude,[2] presumably reflecting only the effect of the rotor/stator interaction. Various degrees of tone steadiness have been observed under various test conditions. By the use of a quantitative measure of tone steadiness useful information concerning the relative tone steadiness associated with various fan test conditions has been obtained.

The results which are presented cover four test conditions. These four test conditions were the following: (1) the typical static condition; (2) operation of the fan with a honeycomb/screen flow control device surrounding the inlet; (3) operation with tunnel flow; and (4) operation with tunnel flow and a cylindrical probe located about 40 probe diameters upstream. These four conditions were chosen to correspond to, respectively, (1) normal ground static fan operation; (2) an approach to flight simulation without forward velocity; (3) simulated flight operation; and (4) simulated flight with an inlet distortion.

Facility and Test Hardware

The facility is extensively described in references 5 and 6. The 9x15 test section is located in the low speed section of one of NASA-Lewis' supersonic wind tunnels. Figure 1 is a sketch of the facility showing the test section in relation to other features of the tunnel facility. This facility, as described in reference 7, permits the simulation of forward flight. The effect of this simulation is that with a flow of 41 m/sec, the test fan's cut-off fundamental blade passage frequency tone was effectively reduced to the level of the surrounding broadband spectrum levels.

The test fan was a 50.8-cm diameter, 1.2-pressure ratio, single stage fan with 15 blades and 25 vanes. Figure 2 presents the front view of the fan in its test position. Figure 3 is a sketch of the fan inlet honeycomb/screen inlet flow control device, showing the details of its construction. Also shown is the location of a probe, which when extended into the fan inlet duct, produced a flow disturbance which contributed to tone noise at the blade passage frequency. The inlet flow control device was intended to smooth the inflow to approach the conditions which might be expected with forward velocity in the wind tunnel or in flight. Figure 4 is a photograph showing the inflow control device.

The noise or sound pressure from the fan was measured at locations both internal and external to the fan nacelle. Outside the fan, at 60° from the inlet axis, a 0.64-cm condenser microphone located at 1.83 m away from the fan monitored the outside level. In addition, several fan wall mounted pressure transducers were used to measure the noise upstream and downstream of the fan. These transducers were 0.2 cm diameter strain gage type dynamic sensors. One inlet pressure transducer and aft pressure transducer will be used to

represent measurements of forward and aft sound pressure.

Test Conditions

The results from a total of four test conditions will be reported. At each inflow condition, the fan was operated along a single operating line at 60, 80, 96, 110, and 115 percent of the 8020 rpm design speed. The first condition was that of the standard ground static inflow with a clean unobstructed inlet. This clean inlet, $V_\infty = 0$ condition duplicates the typical way of testing fans on the ground, with the airflow being drawn nearly spherically from the atmosphere and accelerated through greatly contracting stream tubes into the inlet.

The second condition used the aft blocked inlet flow control device in an attempt to simulate flight fan noise generation without tunnel flow. The outside honeycomb was chosen to reduce the transverse component of the incoming air turbulence and the backing screen was chosen so as to dissipate turbulence created by the honeycomb itself.

The third condition is that of the flight simulation by operating the fan with tunnel flow. This clean inlet, with $V_\infty = 41$ m/sec tunnel flow has been observed to produce fan noise characteristics similar to those measured in flight.[7] The apparent cut-off of the inlet tone due to rotor/stator interaction is in accordance with the Tyler-Sofrin[8] theory predicting nonpropagation for this fan's fundamental tone at speeds less than design, given the particular numbers of rotor and stator blades used here. The second harmonic was cut-on at all speeds at which the fan was tested.

The fourth condition used a 0.64-cm diameter probe inserted into the airstream to produce a flow disturbance which generated noise at the blade passage frequency. With the rod inserted, the tunnel was operated at $V_\infty = 41$ m/sec to remove the random external turbulence and inflow disturbances associated with static fan operation.

Data Processing

Definition of Tone Steadiness

The measure of tone steadiness applied in this paper is derived from the probability density function as measured in a narrow band of frequencies around the tone. The probability density function, or PDF, is the probability distribution of signal amplitudes as a function of amplitude. Any zero mean signal, in this context the measured tone sound pressure, ranges in level over a span of negative to positive levels. The shape of the PDF describing the probability of finding the tone amplitude in any small amplitude range can be interpreted in terms of the relative amounts of steady sinusoidal and unsteady random signal components present.

Cut-on fan tones have been observed to be steady in flight measurements[2] and generally unsteady in ground static testing. To enable the application of the probability density function; a steady tone amplitude can be considered to be modeled by a sine wave. Conversely, a tone that is unsteady, by comparison, has a level that varies randomly with time and the amplitudes are assumed to be distributed in a Gaussian way with the familiar normal probability function. A tone that is a combination, that is, partially steady and partially unsteady, has a PDF that shares, by superposition, the characteristics of both the steady periodic tone and unsteady random noise.

Figure 5 shows some actual waveforms and their associated PDF's. A steady, sinusoidal tone (fig. 5(c)) has the PDF of figure 5(d). The random waveform such as figure 5(e) has its corresponding PDF represented by figure 5(f). The typical noise generated at some particular blade passage frequency, will share these characteristics and can be considered as having a sinusoidal and a random component. The ratio of the mean square value of the sinusoidal, (σ_s^2), to random, (σ_n^2), components, called a steadiness ratio R can be determined from the shape of the PDF by defining a quantity called the probability density ratio or PDR. The PDR is defined as the ratio of the peak PDF value to the value at zero amplitude. This approach was used by Piersol in reference 9. Rice[10] expresses this joint probability density function of sinusoidal and random components as

$$\text{PDF} = \frac{1}{\pi\sqrt{2\pi}\sigma_n} \int_0^\pi e^{-(I-\sqrt{2}\,\sigma_s \cos\theta)^2/2\sigma_n} \, d\theta$$

in which I is the total level. The relationship between R and PDR is displayed in figure 6. The PDF defined above has a maximum at other than zero amplitude only for values of R greater than about 1.8. Therefore, R values less than about 1.8 are indeterminate with the PDR technique.

PDF Determination

The probability density functions were obtained by using a special purpose digital computer to process the pressure data after first isolating the tones with a narrow band filter. In the process, the signal was first digitized to a fine resolution, and then the number of times that each small range of levels was detected was plotted as a function of level. The data were supplied from FM recorded magnetic tapes. The filters that were used to isolate the tones were 10 Hz and 50 Hz wide. Because of variations in fan speed and tape recorder speed, a frequency tracking option on the filter unit was also used so that changes in speed would not take the fan tone frequency outside the filter band. Because of limitations in the rate at which the tracking filter would relocate the band to follow the tone frequency, it was necessary to increase the 10 Hz bandwidth used for PDF measurements of the blade passage frequency to a 50 Hz bandwidth for PDF measurements of the second harmonic.

In generating the probability function, some precautions are in order. These are, in general, concerns with respect to bandwidth and averaging time appropriate in processing any random data. The desirable goals of fine frequency resolution and high confidence in the repeatability of the measurement must be traded off. The standard deviation of the measurement is proportional to $1/\sqrt{BT}$ [11] in which B is the bandwidth of the

data (Hz) and T is the length of the data record (sec). A small frequency bandwidth must be used in isolating the fan frequency tone under consideration so that as little broadband random noise as possible is permitted to dilute the effect of the fan tone noise, which was the quantity of interest in this study. However, a sufficient amount of time (T) must be allowed for the PDF to become consistent. This time is limited by the original fan test requirements. For a given standard deviation or confidence level, the minimum filter bandwidth is determined by the length of the magnetic tape record.

If a filter is chosen for the PDF determination of a tone, and the filter is too narrow for the available averaging time, the resulting PDF will always resemble that of a sine wave, with an unrepeatable PDR. A useful experimental check to insure that the filter width was large enough for the available time was to compute the PDF for white noise and verify that the resulting PDF was Gaussian. The filters chosen for this study had bandwidths at least 250 times the inverse of the record time.

When the fan tone level is not much greater than the broadband level at nearby frequencies, the determination of a ratio of steady to unsteady tone components is difficult. For some of the data points reported this may have been a problem since there was insufficient processing time to permit use of finer resolution filtering. Of course, if a tone was reduced to the background level, a sine wave PDF would never be obtained.

Results and Discussion

The test fan was operated at several speeds with the four inflow conditions. In the following presentation, the individual spectra (6 Hz resolution) and PDF curves for a single speed will be discussed in detail, and then the steadiness ratios (R's) for the various conditions will be compared.

Figures 7 to 10 present the (a) 60° far field microphone spectra and (b) blade passage and (c) second harmonic tone probability density functions at 96 percent fan speed for the four inflow conditions of static, inlet flow control device, full tunnel flow and inlet disturbance rod. Figures 11 to 14 present similar results for an inlet wall-mounted pressure transducer and figures 15 to 18 present similar results for an aft wall-mounted pressure transducer. For this fan, 96 percent speed is below the speed at which the blade passage frequency tone due to rotor/stator interaction propagates. Other tone noise sources at this frequency may be present at any speed.

On examination of figure 7(a) which shows the clean inlet, static flow data for the far field microphone, one can see the prominant BPF and 2 BPF tones in the spectrum. The PDF's for these two tones show an approximately equal steady and random signal content for the BPF (fig. 7(b)), and a somewhat more steady 2 BPF as indicated by the PDF of figure 7(c). The average of the two peak PDF values was used along with the previously discussed PDR evaluation technique to determine the R values marked on the individual PDF figures, and tabulated in Table I. The aft-blocked honeycomb/screen inflow control device, with no tunnel flow exhibits a somewhat reduced BPF. The accompanying PDF's of figures 8(b) and (c) show that the reduced inflow distortion has made the BPF tone more steady, and even the 2 BPF tone has become steadier. Reference to Table I which lists the particular values of steadiness ratio indicates that the BPF tone is nearly an order of magnitude more steady and that the 2 BPF tone is about three times steadier than for the clean inlet condition. When the tunnel flow is used to simulate flight, the sound pressure level spectrum in figure 9(a) shows the almost complete reduction of the BPF tone. Its exact PDR value is questionable because of the relatively small difference in level between the tone and the broadband (fig. 9(a)), but the tone appears random. In the speed range where the fundamental rotor/stator interaction tone was cutoff, reference 2 showed PDF's for the residual tone in flight which were either random or somewhat steady depending on the proximity of the tone to the broadband level. The second harmonic has become extremely steady (fig. 9(c)), as measured by the steadiness ratio of 164. The results when the inlet rod was inserted in conjunction with tunnel flow show that again a blade passage frequency tone is generated along with the 2 BPF tone (fig. 10(a)), but that, as might be expected with a spatially fixed distortion, the tones are very steady (figs. 10(b) and (c)). From the PDF's, steadiness ratios of 50 to 60 are indicated.

The effects of the different flow conditions on the fan tones as sensed by the inlet transducer are generally similar to those of the previously discussed external microphone. However, the tones were generally less steady in the inlet than they were in the external acoustic field, perhaps because of boundary layer turbulence. Spectra for the four inflow conditions (figs. 11(a) to 14(a)) are very similar to the corresponding spectra for the microphone. However, for the first static condition, the amplitude distributions (figs. 11(b) and (c)) of the two tones appear mostly random; and with inflow control, only the second harmonic (fig. 12(c)) has been made steady. With tunnel flow and the clean inlet, the upstream transducer senses an extremely steady 2 BPF tone (fig. 13(c)) and a BPF tone which, as before, has a questionable PDR. Inserting the distortion rod (fig. 14) into the inlet produced a ratio of 5 to 7 at 96 percent speed.

To complete the presentation at 96 percent speed, the results from the downstream wall-mounted transducer are shown in figures 15 to 18. For the clean inlet, static condition, the fan tones were observed to be unsteady. These aft transducer fan tones have an unsteadiness (figs. 15(b) and (c)) resembling that of the inlet transducer (figs. 11(b) and (c)). The general shape of these PDF's appear to indicate a random tone, but do not have the sloping sides of the previously presented Gaussian noise plus sinusoidal distributions. Reference 9 describes a PDF similar to these as being produced by a sine wave whose level is a function of a constant term and some Gaussian noise. In other words, the clean inlet, $V_\infty = 0$ tones seem to be better modeled by a periodic wave at least partially modulated by Gaussian noise (figs. 11(a) and 15(a)), than by a summation of periodic wave and Gaussian noise. The spectra also seem to support this modulation concept for the clean inlet, $V_\infty = 0$ tones as evidenced by the width of the tones. With the addition of inflow control, the BPF tone became

steady, while the second harmonic remained unsteady. With tunnel flow and clean inlet, contrary to what was observed with the inlet and front quadrant noise measurements, the BPF tone was determined to be steady (fig. 17(b)), and the second harmonic (fig. 17(c)) unsteady. With a rod in place to create an inlet disturbance, both fan tones (fig. 18) were relatively steady.

Table I presents the steadiness ratios determined for the other fan speeds. As can be seen, there are some large variations from speed to speed. That there are variations in steadiness from speed to speed may perhaps have been expected as the testing was performed over a period of several weeks with possible variations in tunnel setup and atmospheric conditions from one test point to another.

An average steadiness ratio was calculated for each tone and operating condition. Because of the occasional large variations of steadiness ratio due to the nonlinear PDR to steadiness ratio (R) conversion curve (fig. 6), the PDR's for each value were averaged, and then the average converted to R. The PDR for PDF's having a maximum only at zero amplitude were arbitrarily set equal to 0, and the final average R rounded off to the nearest integer. These results are presented in Table II.

Certain broad conclusions can be drawn from Table II by comparing one inflow condition to another. First, the standard static operation gives rise to the most unsteady fan tones. Second, applying inflow control to the fan can make the tones steadier by about an order of magnitude, particularly as determined outside the fan. The residual tone in the cut-off region of fan speed may become steadier because of some spatially steady inflow distortions introduced by the inflow control device. Conversely, the cut-on frequency tone becomes steadier because of the removal of random turbulence. With tunnel flow the steadiness of the second harmonic tone, at least in the front, can be increased substantially over the values determined by adding inflow control to the static operation. Finally, with the flow disturbance created by the inlet rod, the 2 BPF tones that are produced take on steadiness values (figs. 19 to 21) numerically similar to those of the clean inlet with tunnel flow. That the 2 BPF tone is approximately equally steady with and without the rod implies that the rod's additional contribution as a steady source at that frequency is small. In attempting to explain why the tones are so much more steady outside the duct, a possible explanation is that boundary layer disturbances or pseudosound are sensed by the wall transducers.

In evaluating methods of fan forward flight simulation, it would appear that steadiness of a cut-on fan tone (such as the fan second harmonic in this study) is an indicator of low inlet turbulence. However, when a tone due to rotor/stator interaction is cut-off, any residual tone observed is due to a generation mechanism other than rotor/stator interaction, and could be steady or unsteady depending on the character of the tone producing flow disturbance. Thus the increase in the steadiness of the cut-on second harmonic achieved with the use of the honeycomb/screen inflow control device indicates that its purpose of reducing the random turbulence to flight levels was partially achieved. On the other hand, the increase in the steadiness ratio of the BPF tone in the cut-off regime might indicate that the inflow control device introduced spatially steady inflow distortions. These distortions generated the tone in a manner analogous to the effect of the inlet rod with tunnel flow. For the clean inlet, tunnel flow case, the high levels of second harmonic steadiness (56 at the external microphone and 26 in the inlet) are indicators of the degree of inlet flow conditioning required to produce nearly complete cut-off of the forward radiated fundamental tone.

Summary of Results

The technique of amplitude probability density was used to evaluate the steadiness of fan noise tones that were generated under a variety of fan inflow conditions. The steadiness ratio is the ratio at a given tone frequency of the mean square sinusoidal-to-random components that can be thought of as constituting the tone. For the condition of standard static operation with a clean inlet, the fan tones were found to be only slightly steady. Adding a honeycomb/screen inlet flow control device caused the blade passage frequency and second harmonic tones to become approximately an order of magnitude more steady. With operation of the fan in a clean inlet configuration with a wind tunnel airflow of 41 m/sec, the cut-on, second harmonic tones become about two orders of magnitude more steady than was the case for the static condition. A fourth condition of tunnel air flow with an inlet distortion rod also produced very steady tones.

References

1. Feiler, C. E. and Groeneweg, J. F., "Summary of Forward Velocity Effects on Fan Noise," NASA TM-73722, 1977.

2. Merriman, J. E. and Good, R. C., "Effect of Forward Motion on Fan Noise," AIAA Paper 75-464, Mar. 1975.

3. Shaw, L. M., Woodward, R. P., Glaser, F. W., and Dastoli, B. J., "Inlet Turbulence and Fan Noise Measured in an Anechoic Wind Tunnel and Statically with an Inlet Flow Control Device," AIAA Paper 77-1345, Oct. 1977.

4. Woodward, R. P., Wazyniak, J. A., Shaw, L. M., and MacKinnon, M. J., "Effectiveness of an Inlet Flow Turbulence Control Device to Simulate Flight Fan Noise in an Anechoic Chamber," NASA TM-73855, 1977.

5. Yuska, J. A., Diedrich, J. H., and Clough, N., "Lewis 9- by 15-Foot V/STOL Wind Tunnel," NASA TM X-2305, 1971.

6. Rentz, P. E., "Softwall Acoustical Characteristics and Measurement Capabilities of the NASA Lewis 9x15 Foot Low Speed Wind Tunnel," Bolt, Beranek and Newman, Inc., Canoga Park, Calif., BBN-3176, June 1976. (NASA CR-135026.)

7. Dietrich, D. A., Heidmann, M. F., and Abbott, J. M., "Acoustic Signatures of a Model Fan in the NASA-Lewis Anechoic Wind Tunnel," AIAA Paper 77-59, Jan. 1977.

8. Tyler, J. M. and Sofrin, T. G., "Axial Flow Compressor Noise Studies," SAE Transactions, Vol. 70, 1962.

9. Bliss, D. B., Chandiramani, K. L., and Piersol, A. G., "Data Analysis and Noise Prediction for the QF-1B Experimental Fan Stage," Bolt, Beranek and Newman, Inc., Canoga Park, Calif., BBN-3338, Aug. 1976. (NASA CR-135066.)

10. Rice, S. O., "Mathematical Analysis of Random Data," Selected Papers on Noise and Stochastic Processes, Wax, N., ed., Dover Publications, New York, 1954, pp. 133-294.

11. Bendat, J. S. and Piersol, A. G., Random Data: Analysis and Measurement Procedures, John Wiley & Sons, Inc., 1971.

TABLE I. - STEADINESS RATIOS

[R is mostly random; no data exists for dashed entries.]

Speed (percent of design)	Transducer	Condition and tone							
		Clean inlet V_∞ = 0		Inflow control V_∞ = 0		Clean inlet V_∞ = 41 m/sec		Inlet rod V_∞ = 41 m/sec	
		BPF	2 BPF	BPF	2 BPF	BPF	2 BPF	BPF	2 BPF
60	60° Mike	---	--	240	125	R	30	5	73
	Inlet pressure	---	--	11	R	R	5	4	16
	Aft pressure	---	--	---	---	R	5	R	2
80	60° Mike	6	18	4	6	R	46	83	80
	Inlet pressure	R	5	2	40	R	37	33	72
	Aft pressure	R	R	---	---	5	R	24	R
96	60° Mike	1.8	7	9	22	R	164	50	60
	Inlet pressure	R	R	R	10	R	144	7	5
	Aft pressure	R	R	9	R	13	R	18	10
110	60° Mike	4	R	8	1.8	--	---	42	24
	Inlet pressure	3	R	R	2	--	---	19	7
	Aft pressure	4	2	---	10	--	---	6	34
115	60° Mike	3	R	12	2	R	31	71	46
	Inlet pressure	3	R	R	R	3	8	20	9
	Aft pressure	8	R	---	---	33	16	17	R

TABLE II. - AVERAGE STEADINESS RATIOS

Transducer	Condition and tone							
	Clean inlet V_∞ = 0		Inflow control V_∞ = 0		Clean inlet V_∞ = 41 m/sec		Inlet rod V_∞ = 41 m/sec	
	BPF	2 BPF	BPF	2 BPF	BPF	2 BPF	BPF	2 BPF
60° Mike	3	1	18	13	[a]R	56	41	54
Inlet pressure	<1.8	R	<1.8	<1.8	[a]R	26	14	14
Aft pressure	<1.8	R	----	----	5	<1.8	6	<1.8

[a]These two values are questionable.

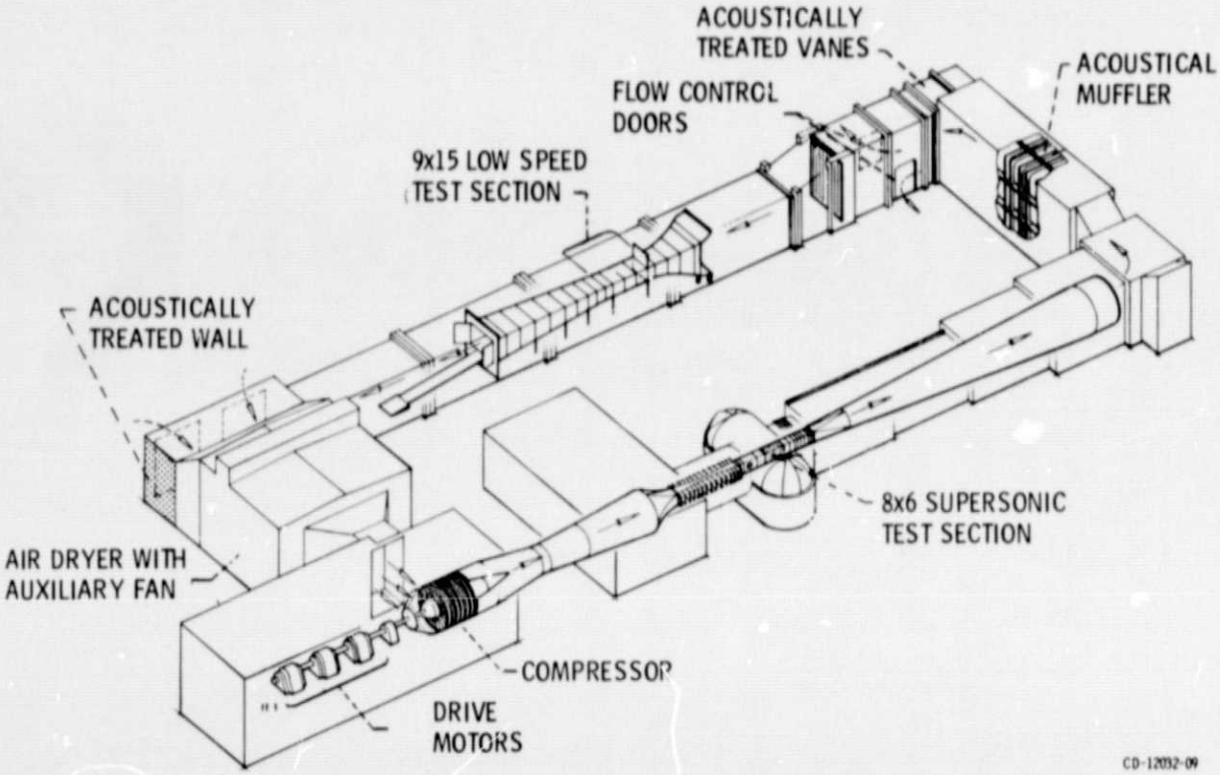

Figure 1. - The NASA-Lewis 8- by 6-foot and 9- by 15-foot wind tunnels.

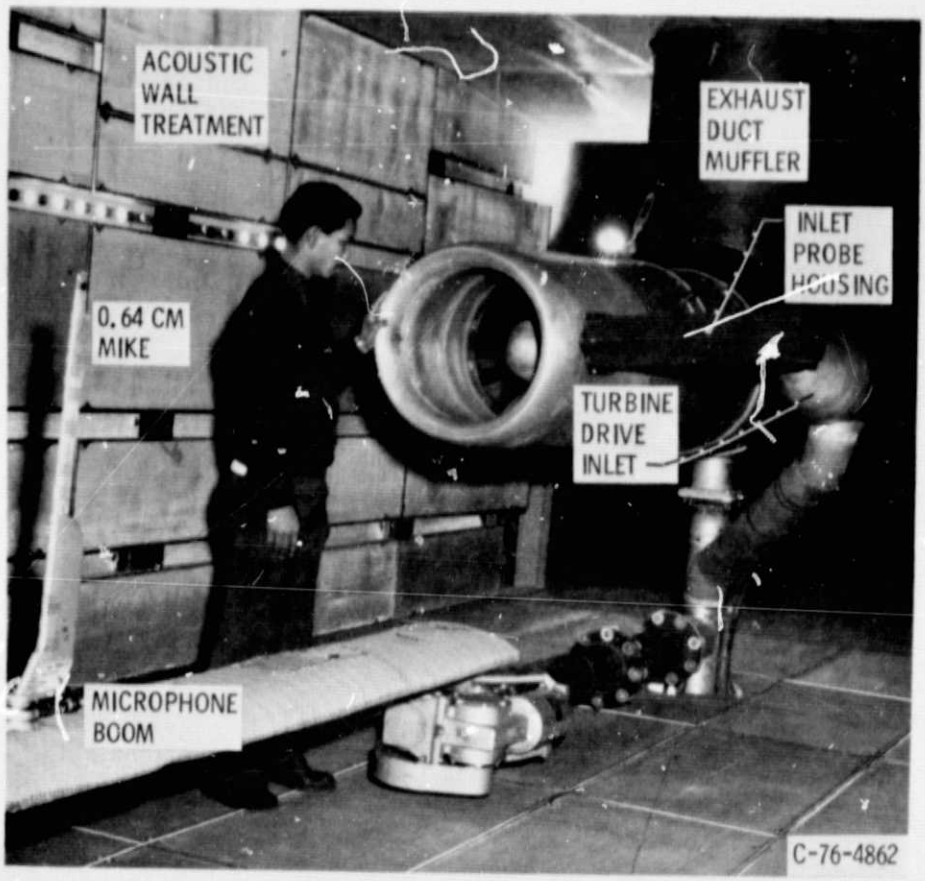

Figure 2. - Upstream view of simulator in anechoic tunnel.

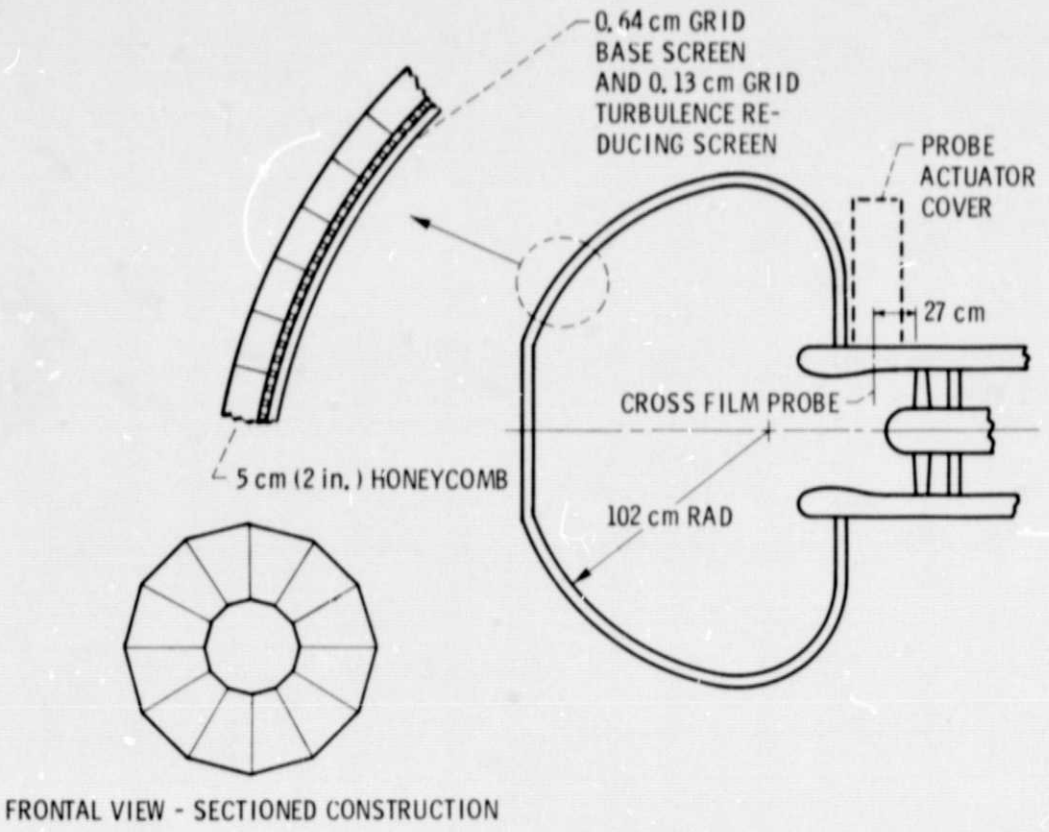

E-7621

Figure 3. - Inlet flow control device.

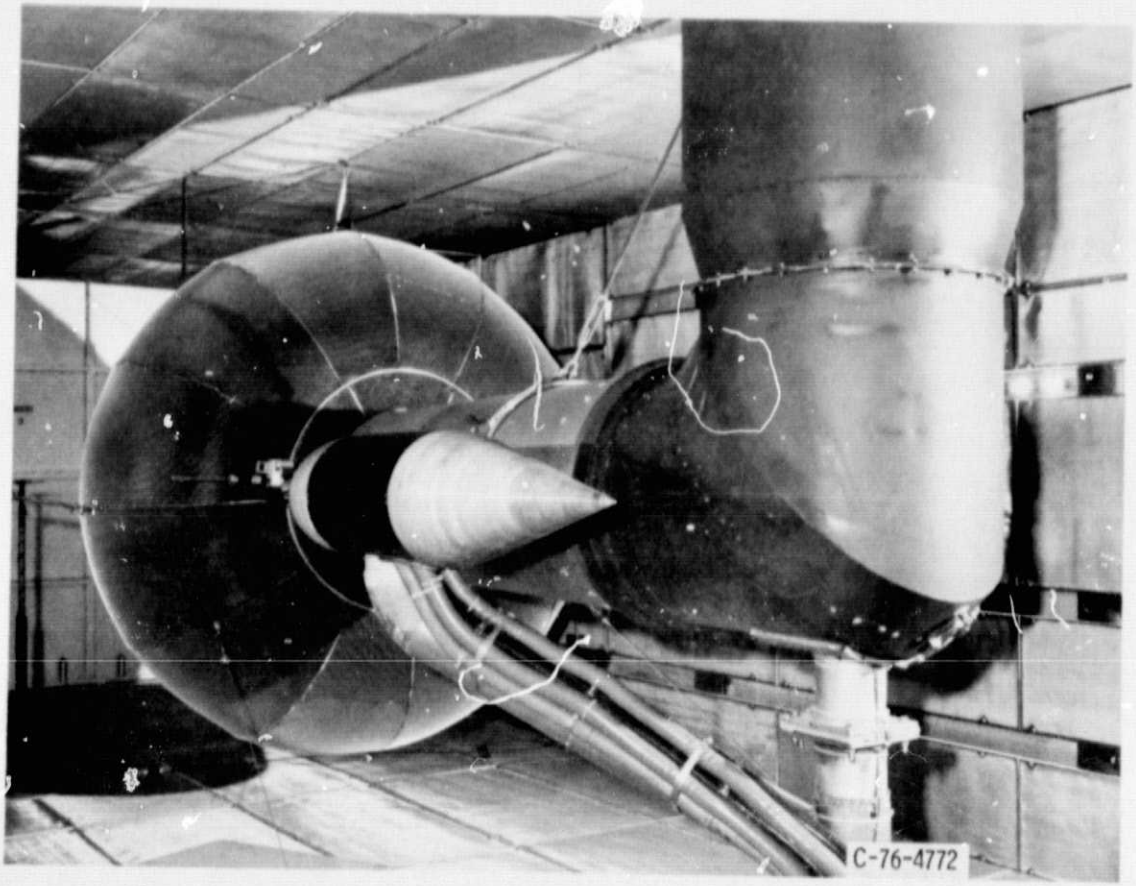

Figure 4. - Aft view of simulator showing inlet honeycomb cage in place.

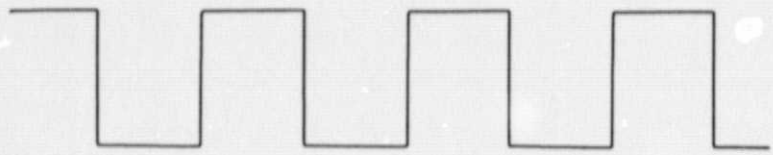

(a) SQUARE WAVE.

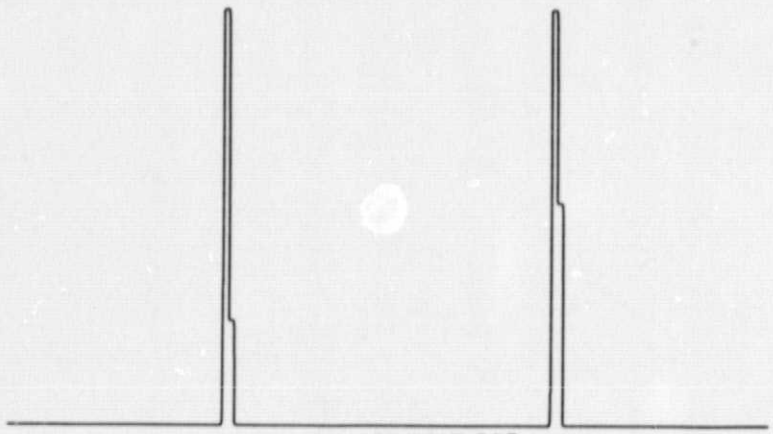

(b) SQUARE WAVE PDF.

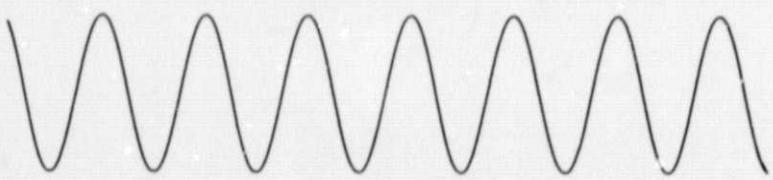

(c) SINE WAVE.

Figure 5.

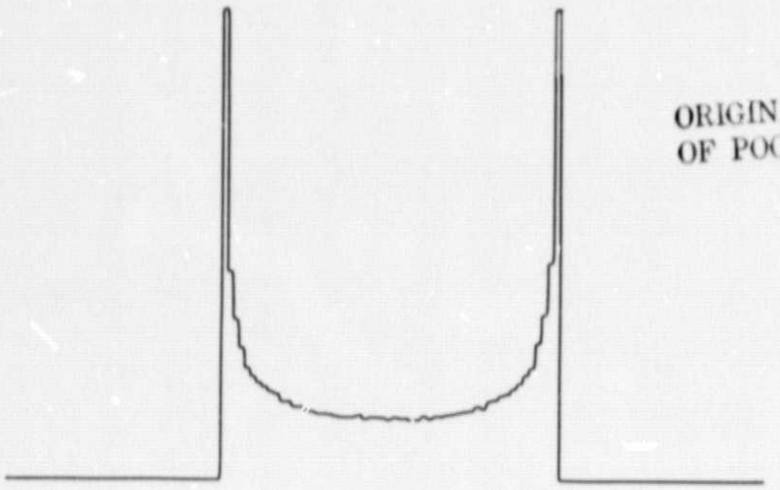

(d) SINE WAVE PDF.

(e) WHITE NOISE.

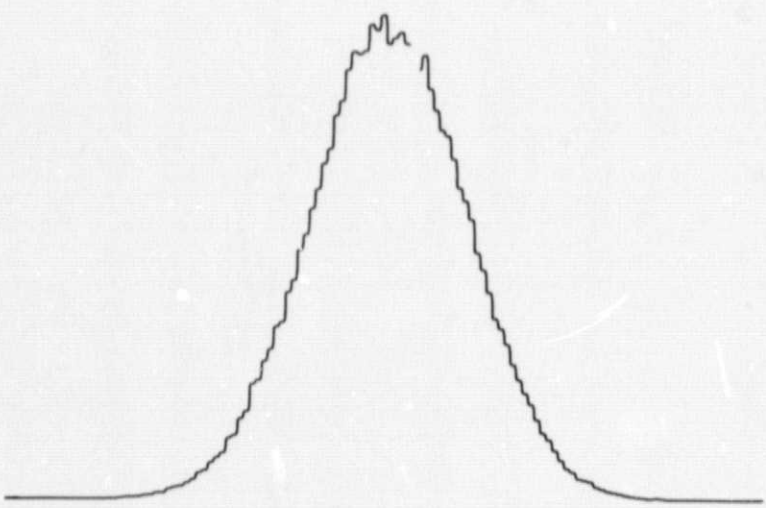

(f) GAUSSIAN (WHITE NOISE) PDF.

Figure 5. - Concluded.

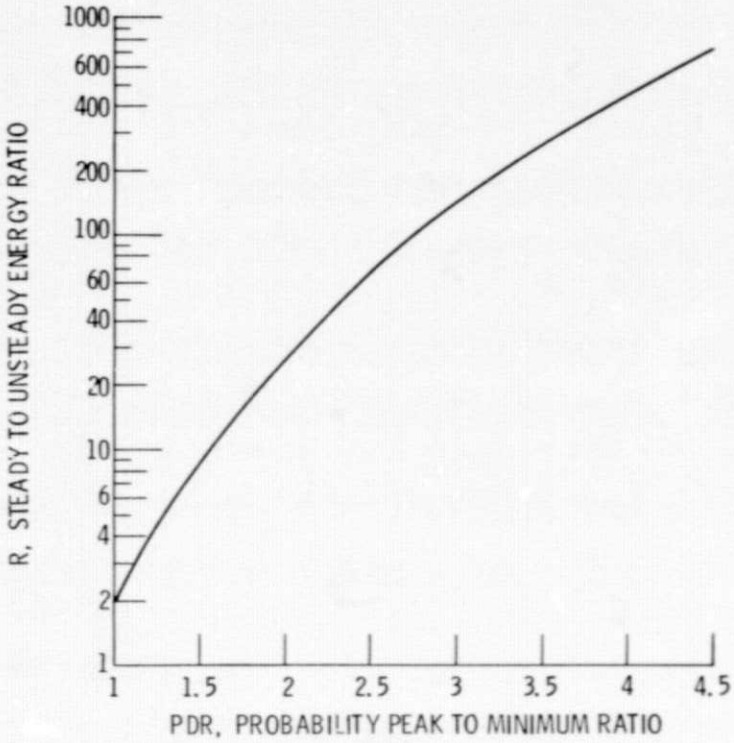

Figure 6. - PDR to R conversion.

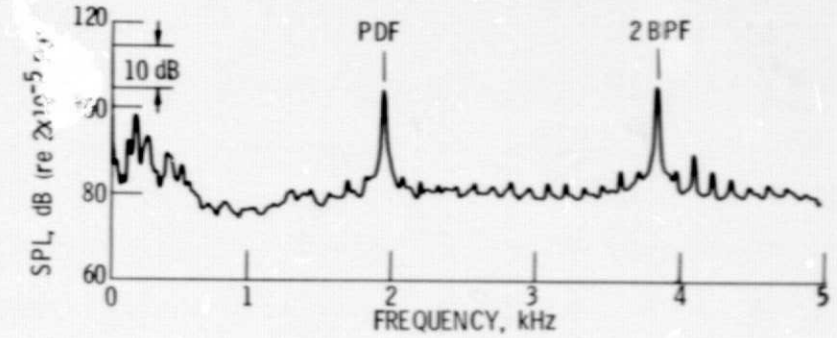

(a) SPECTRUM.

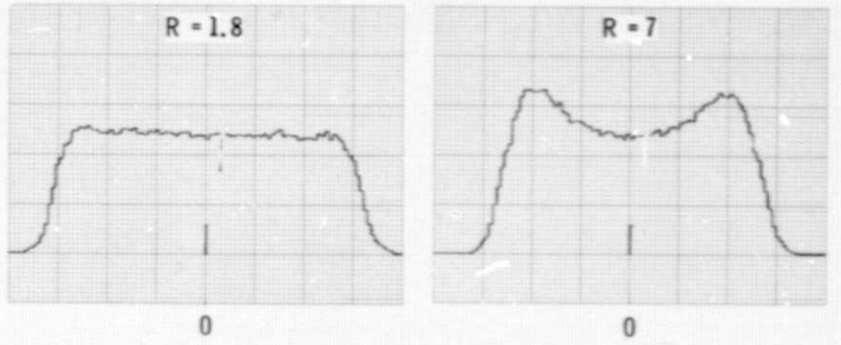

(b) BLADE PASSAGE FREQUENCY PDF.

(c) BLADE PASSAGE FREQUENCY SECOND HARMONIC PDF.

Figure 7. - Spectrum and probability density functions for the 60° microphone at the clean inlet, V_∞ = 0 condition.

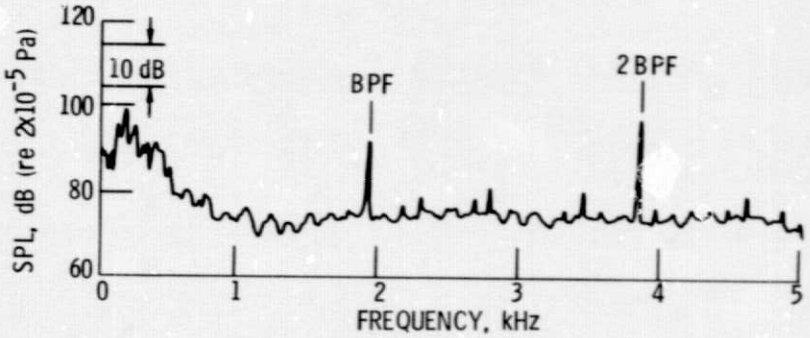

(a) SPECTRUM.

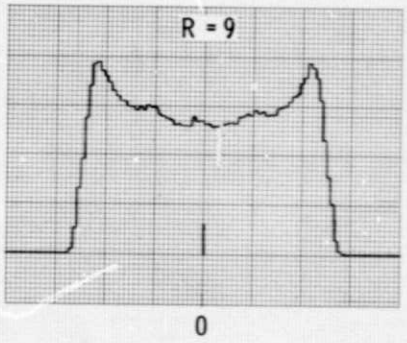

(b) BLADE PASSAGE FREQUENCY PDF.

(c) BLADE PASSAGE FREQUENCY SECOND HARMONIC PDF.

Figure 8. - Spectrum and probability density functions for the 60° microphone at the inflow control, V_∞ = 0 condition.

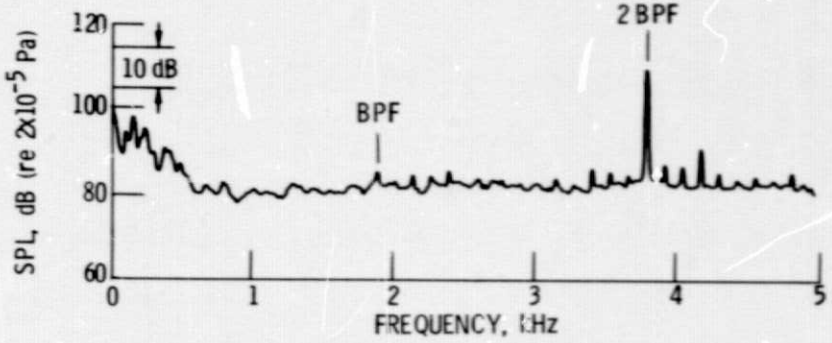

(a) SPECTRUM.

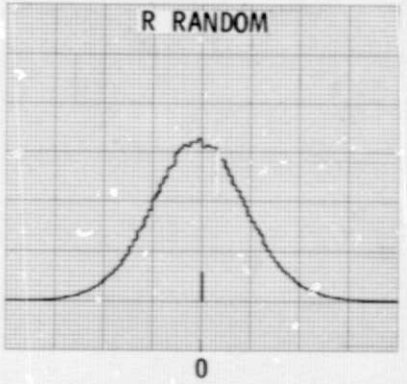

(b) BLADE PASSAGE FREQUENCY PDF.

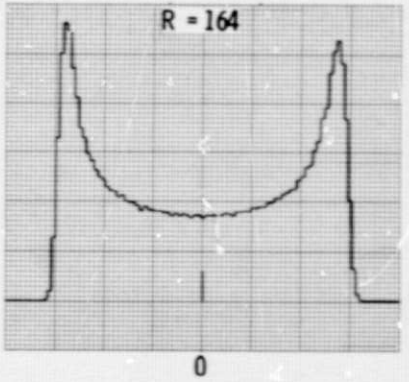

(c) BLADE PASSAGE FREQUENCY SECOND HARMONIC PDF.

Figure 9. - Spectrum and probability density functions for the 60° microphone at the clean inlet, V_∞ = 41 m/sec condition.

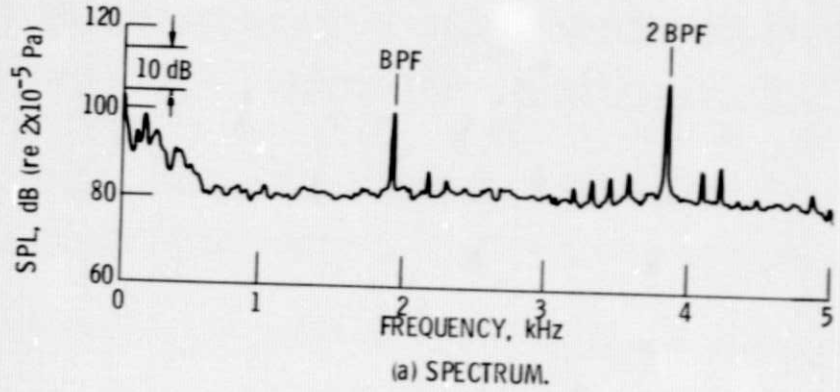

(a) SPECTRUM.

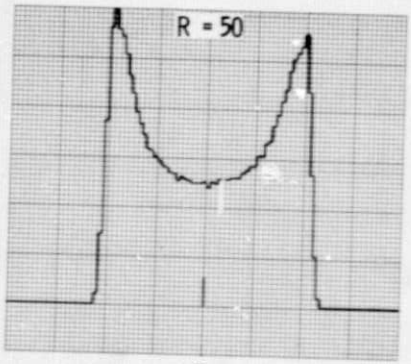

(b) BLADE PASSAGE FREQUENCY PDF.

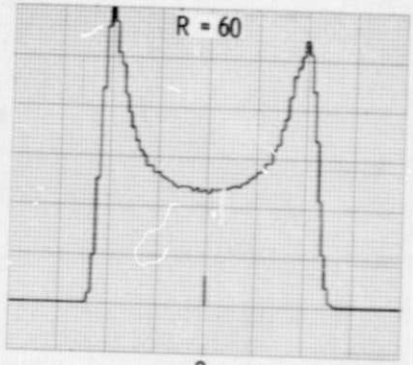

(c) BLADE PASSAGE FREQUENCY SECOND HARMONIC PDF.

Figure 10. - Spectrum and probability density functions for the 60° microphone at the inlet rod, V_∞ = 41 m/sec condition.

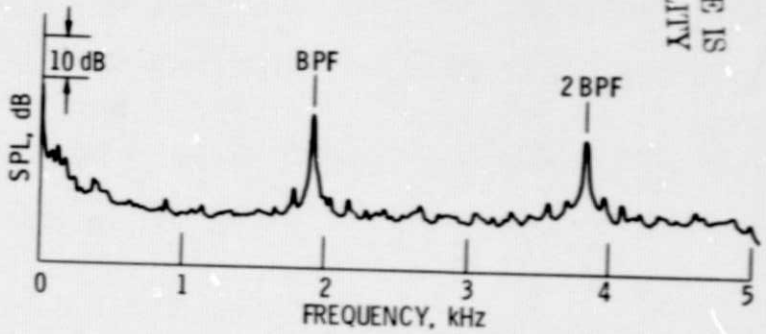

(a) SPECTRUM.

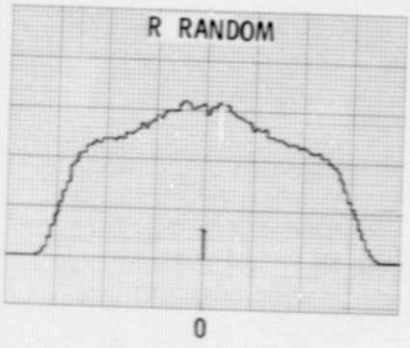

(b) BLADE PASSAGE FREQUENCY PDF.

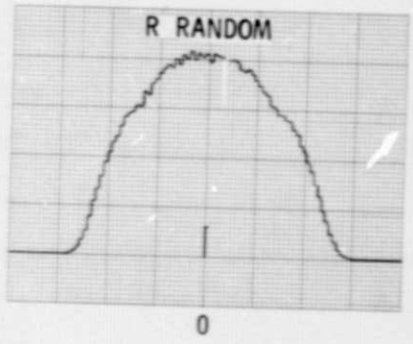

(c) BLADE PASSAGE FREQUENCY SECOND HARMONIC PDF.

Figure 11. - Spectrum and probability density functions for the inlet transducer at the clean inlet, V_∞ = 0 condition.

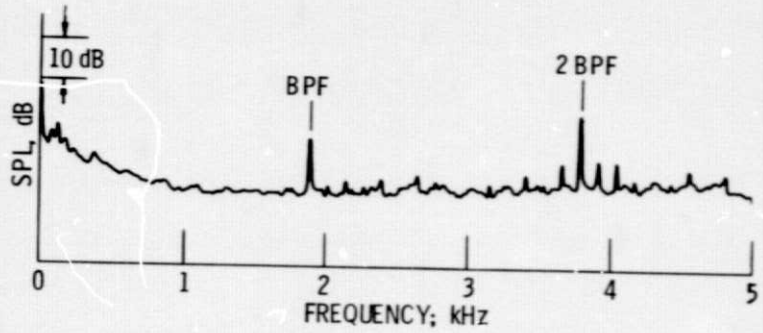

(a) SPECTRUM.

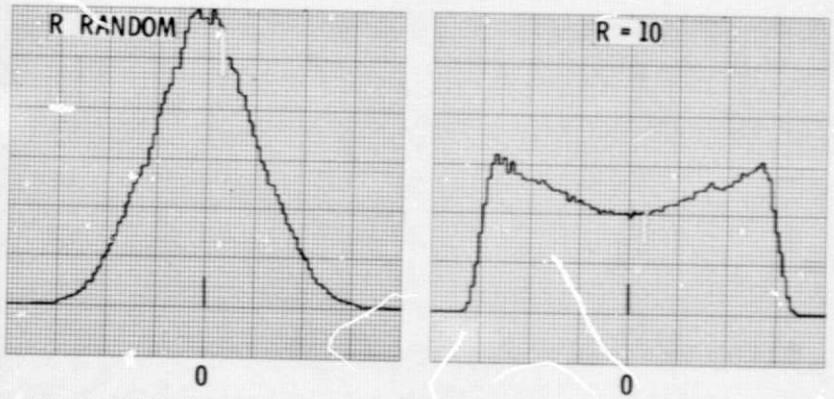

(b) BLADE PASSAGE FREQUENCY PDF.

(c) BLADE PASSAGE FREQUENCY SECOND HARMONIC PDF.

Figure 12. - Spectrum and probability density functions for the inlet transducer at the inflow control, $V_\infty = 0$ condition.

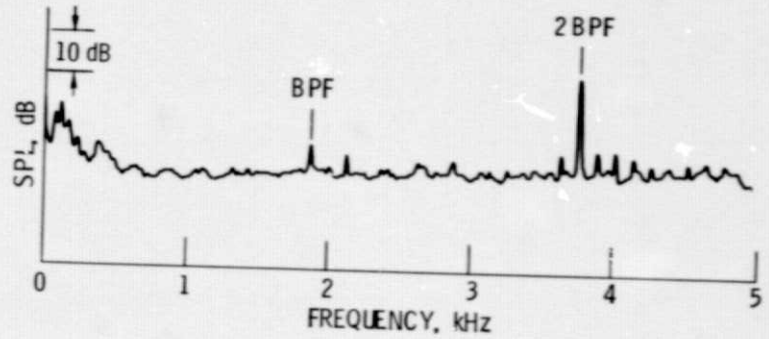

(a) SPECTRUM.

(b) BLADE PASSAGE FREQUENCY PDF.

(c) BLADE PASSAGE FREQUENCY SECOND HARMONIC PDF.

Figure 13. - Spectrum and probability density functions for the inlet transducer at the clean inlet, $V_\infty = 41$ m/sec condition.

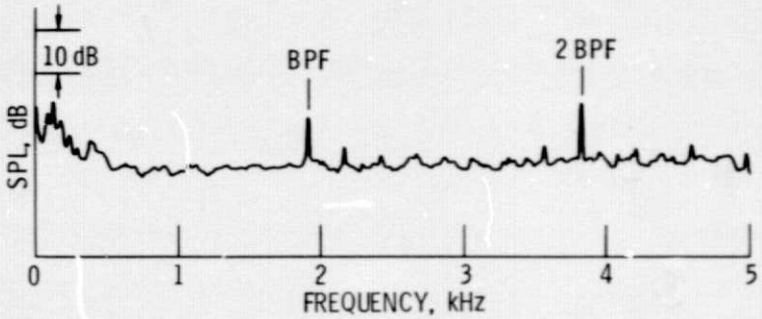

(a) SPECTRUM.

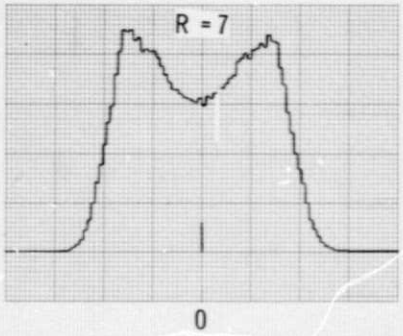

(b) BLADE PASSAGE FREQUENCY PDF.

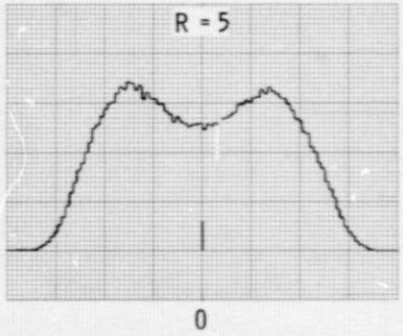

(c) BLADE PASSAGE FREQUENCY SECOND HARMONIC PDF.

Figure 14. - Spectrum and probability density functions for the inlet transducer at the inlet rod, V_∞ = 41 m/sec condition.

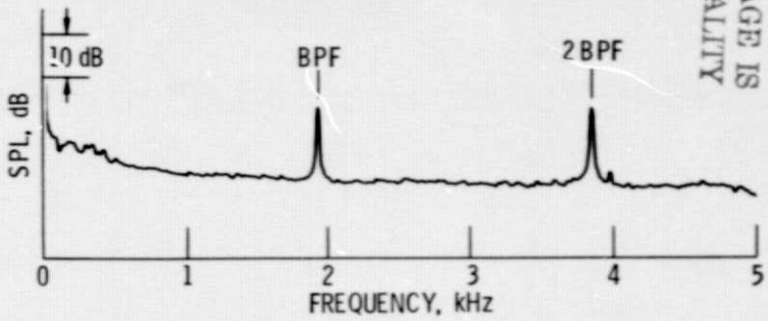

(a) SPECTRUM.

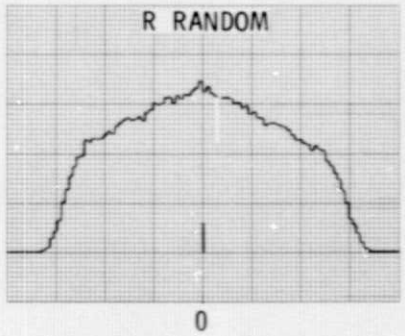

(b) BLADE PASSAGE FREQUENCY PDF.

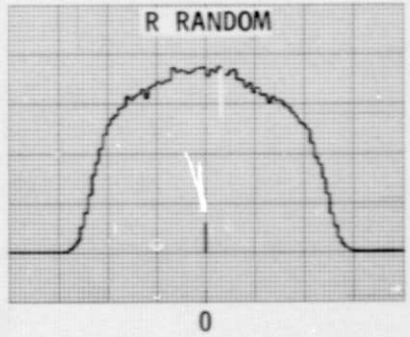

(c) BLADE PASSAGE FREQUENCY SECOND HARMONIC PDF.

Figure 15. - Spectrum and probability density functions for the aft transducer at the clean inlet, V_∞ = 0 condition.

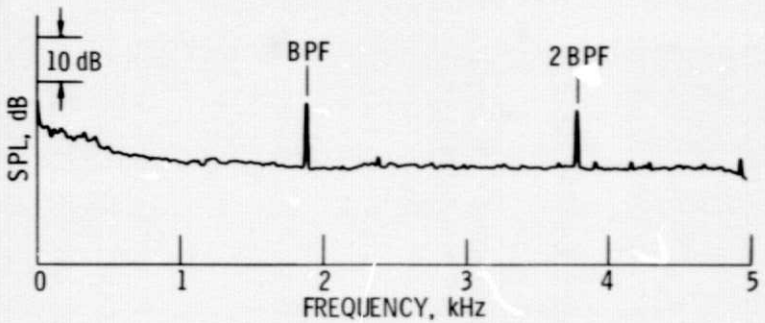

(a) SPECTRUM.

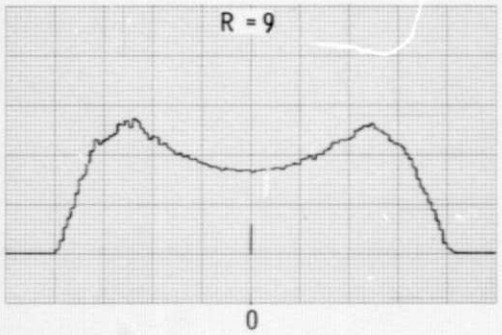

(b) BLADE PASSAGE FREQUENCY PDF.

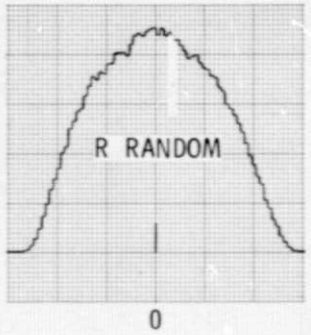

(c) BLADE PASSAGE FREQUENCY SECOND HARMONIC PDF.

Figure 16. - Spectrum and probability density functions for the aft transducer at the inflow control, V_∞ = 0 condition.

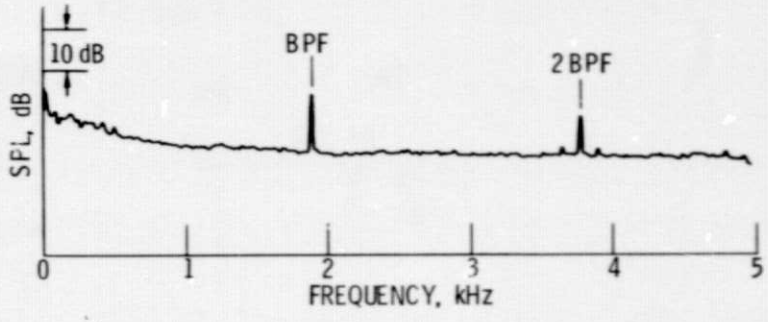

(a) SPECTRUM.

(b) BLADE PASSAGE FREQUENCY PDF.

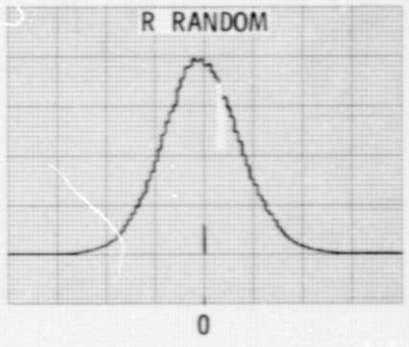

(c) BLADE PASSAGE FREQUENCY SECOND HARMONIC PDF.

Figure 17. - Spectrum and probability density functions for the aft transducer at the clean inlet, V_∞ = 41 m/sec condition.

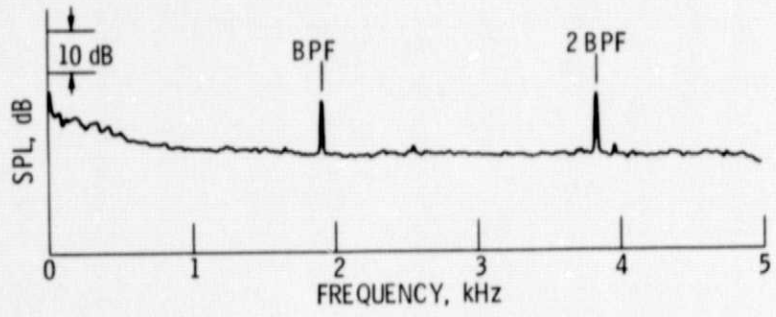

(a) SPECTRUM.

(b) BLADE PASSAGE FREQUENCY PDF.

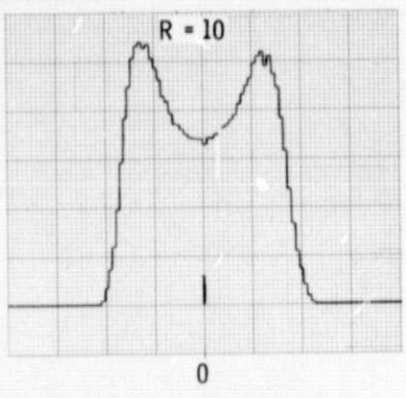

(c) BLADE PASSAGE FREQUENCY SECOND HARMONIC PDF.

Figure 18. - Spectrum and probability density functions for the aft transducer at the inlet rod, V_∞ = 41 m/sec condition.